Jurnal Teknologi

Full Paper

# ENHANCED RULE-BASED ENERGY MANAGEMENT STRATEGY FOR A PHOTOVOLTAIC-WIND-BATTERY-DIESEL STANDALONE MICROGRID CONSIDERING DEMAND RESPONSE PROGRAM

Ng Rong Wee, Jasrul Jamani Jamian*, Syed Norazizul Syed Nasir, Norazliani Md Sapari

Faculty of Electrical Engineering, Universiti Teknologi Malaysia, 81310 UTM Johor Bahru, Johor, Malaysia

**Article history**
Received
*22 May 2024*
Received in revised form
*6 September 2024*
Accepted
*17 September 2024*
Published Online
*28 April 2025*

*Corresponding author
jasrul@fke.utm.my

## Graphical abstract

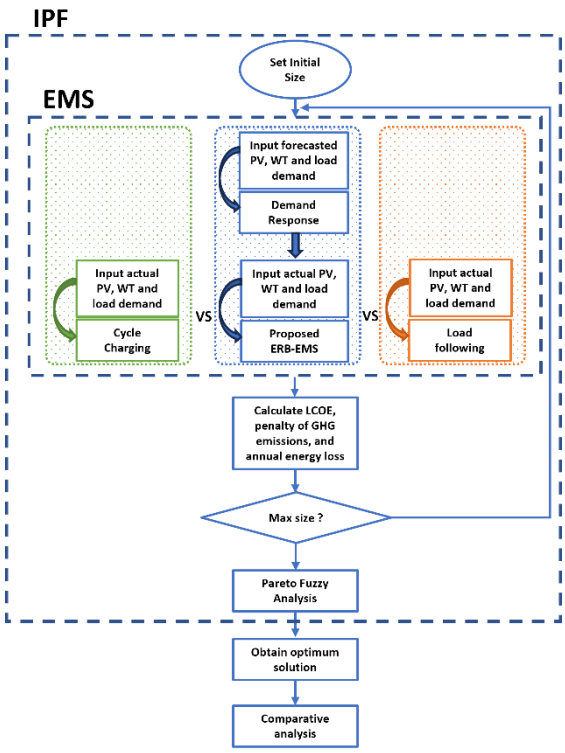


## Abstract

A robust energy management strategy is essential for microgrid operations due to the intermittent nature of renewable energy sources. This paper introduces the Enhanced Rule-Based Energy Management Strategy (ERB-EMS) for a photovoltaic-wind-battery-diesel standalone microgrid. The ERB-EMS integrates a day-ahead load shifting mechanism and an intra-day dispatch method to reduce reliance on conventional generators, thereby lowering costs and greenhouse gas emissions. The scheduling process begins day-ahead, with the system identifying periods of excess renewable energy generation and unmet load, and schedules load shifting accordingly. On the next day, real-time adjustments based on day-ahead planning and operational constraints are made. Simulation results from a case study conducted on the remote island of Ouessant show that ERB-EMS reduces diesel generator utilization from 228,150 kWh to 106,373 kWh, compared to the cycle charging (CC) and load following (LF) strategies. Finally, configuration optimization using the Iterative-Pareto-Fuzzy (IPF) under different energy management strategies, considering the levelized cost of energy (LCOE), penalty for greenhouse gas (GHG) emission, and annual internal energy loss of microgrid components, demonstrates that ERB-EMS outperforms other strategies. With an LCOE of 0.205 $/kWh, a GHG emissions' penalty of $2,220, and an energy loss of 69,537 kWh, ERB-EMS proves to be an effective solution for reducing costs and emissions in microgrid operations.

*Keywords*: Microgrid sizing, rule-based energy management strategy, standalone microgrid, load shifting, demand response

## Abstrak

Strategi pengurusan tenaga yang kukuh adalah penting bagi pengoperasian grid mikro kerana sifat ketidaktentuan sumber tenaga boleh diperbaharui. Kertas kerja ini memperkenalkan Strategi Pengurusan Tenaga Berasaskan Peraturan Diperkukuh (ERB-EMS) untuk grid mikro tersendiri yang menggabungkan mekanisma peralihan beban awal-sehari dan kaedah pengagihan intrahari bagi mengurangkan kebergantungan pada sumber tenaga konvensional, lalu menurunkan kos dan pelepasan gas rumah hijau. Proses penjadualan bermula awal-sehari, dengan sistem mengenalpasti tempoh masa dimana penjanaan tenaga boleh diperbaharui berlebihan dan beban yang tidak dipenuhi, lalu menjadualkan peralihan beban sewajarnya. Pada hari berikutnya,

penyesuaian masa nyata dibuat berdasarkan perancangan hari sebelumnya dan sekatan pengoperasian. Keputusan simulasi dari kajian kes yang dijalankan di pulau terpencil Ouessant menunjukkan bahawa ERB-EMS mengurangkan penggunaan penjana diesel dari 228,150 kWh kepada 106,373 kWh, berbanding dengan strategi penukaran kitaran (CC) dan pengikut beban (LF). Akhirnya, pengoptimuman konfigurasi menggunakan Iterative-Pareto-Fuzzy (IPF) di bawah strategi pengurusan tenaga yang berbeza, dengan mengambil kira kos tenaga terimbang (LCOE), penalti pelepasan gas rumah (GHG) hijau, dan kehilangan tenaga dalaman tahunan komponen grid mikro, menunjukkan bahawa ERB-EMS mempunyai kelebihan berbanding strategi lain. Dengan LCOE sebanyak 0.205 $/kWh, penalti pelepasan gas rumah hijau sebanyak $2220, dan kehilangan tenaga sebanyak 69,537 kWh, ERB-EMS terbukti sebagai penyelesaian yang berkesan untuk mengurangkan kos dan pelepasan gas rumah hijau dalam operasi grid mikro.

*Kata kunci*: Saiz grid mikro, sistem pengurusan tenaga berasaskan peraturan, grid mikro tersendiri, peralihan beban, respon permintaan



## 1.0 INTRODUCTION

The increasing greenhouse gas (GHG) emissions from electricity generation have led to environmental issues such as global warming and climate change. In the United States, approximately 25% of cumulative GHG emissions stem from the energy sector [1]. Consequently, considerable research efforts have been devoted to exploring alternatives to traditional electricity generation methods, and renewable energy resources emerge as a promising solution. However, the intermittent nature of renewable energy generation poses a significant challenge.

To address the intermittency challenge, energy storage systems (ESSs) are integrated into renewable energy systems, creating an independent grid system known as a microgrid. A microgrid can operate in either grid-connected or standalone mode, with the latter being ideal for isolated and remote regions where access to the main power grid is lacking. In standalone microgrids, conventional generators, such as diesel generators (DGs), are often used as backup power sources. Given the diverse characteristics of various energy sources interconnected within a grid system, adopting an efficient energy management strategy (EMS) is vital to ensure economical and reliable microgrid operation.

The main objective of EMS design is to ensure reliable operation while minimizing the cost and emissions of the microgrid. Hence, a well-designed EMS should achieve these objectives by maximizing the use of renewable energy sources (RES), thereby reducing the need for conventional generators. Additionally, consumer participation could improve the flexibility of microgrid operation and further contribute to achieving the objectives.

Over the years, several EMSs have been proposed for standalone microgrid sizing. Research conducted by Raya-Armenta *et al*. [2] provides an insightful review of these EMS approaches. Generally, EMSs can be categorized into optimization-based and rule-based EMSs. An optimization-based EMS aims to identify the best combination of solutions by minimizing or maximizing specific parameters, such as cost, emissions, and reliability. On the other hand, rule-based EMS (RB-EMS) operates based on predefined rules that simplify system operation. While numerous optimization-based EMSs have been proposed by researchers [3-7], RB-EMS has garnered interest among researchers focused on microgrid planning. RB-EMS offers the advantages of operational simplicity, reduced computational time, suitability for real-time applications, and the ability to provide exact solutions to energy management problems.

RB-EMSs generally prioritize RESs during dispatch. When RESs are unable to meet the load demand, the ESSs are discharged, and in cases of excessive renewable energy generation, the surplus power is used to charge the ESSs. Conventional generators serve as backup power sources in these systems. However, specific approaches are employed to tackle problems related to insufficient and excessive power generation. Popular methods include cycle charging (CC) and load following (LF) strategies. Under the CC method, conventional generators run at their rated power when activated [8, 9]. The drawback of CC dispatch is its high operating cost due to running conventional generators at full capacity regardless of the power deficit. In contrast, the LF strategy allows conventional generators to supply just enough power to meet the load demand whenever RESs and ESSs are unable to cover it [10-13]. However, the LF strategy may underutilize ESSs as they may not be adequately recharged after usage. Excessive power generation is often curtailed or diverted to dump loads.

The CC and LF strategies are so popular that they are readily available in energy resource optimization software such as HOMER. However, several researchers have modified the existing algorithms and systems to improve performance. Mukhtaruddin *et al*. [14] proposed

a microgrid system with photovoltaic (PV) panels, wind turbines (WTs), and ESSs, where conventional generators are not installed. While this system ensures zero GHG emissions, it is too dependent on RESs and lacks backup energy resources to manage the uncertainties associated with RESs.

In studies related to grid-connected (GC) microgrids, the decision to import or export power from the utility grid is considered when designing an RB-EMS. Alsharif *et al*. [15] and Hakimi *et al*. [16] both proposed an RB-EMS for a GC microgrid.

Demand response is another important aspect in EMSs that is still lacking in microgrid sizing studies. Mohandes *et al*. [17] proposed a load shifting mechanism for a standalone microgrid consisting of a thermal energy storage system, while Mukhopadhyay and Das [18] proposed a demand response program for a grid-tied microgrid. Conversely, Candra [19] considered load shedding in the study of optimal sizing of hybrid energy resources.

In microgrid sizing studies, cost has become the primary focus. Zhu *et al*. [20] aimed to determine the optimal size of an islanded hybrid microgrid system that minimizes the annualized cost of the system. Bukar *et al*. [8] proposed the Grasshopper Optimization Algorithm for sizing a PV, WT, and battery microgrid to minimize the levelized cost of energy (LCOE). A more recent study by Khawaja [21] optimized the size of a standalone PV-BES microgrid using an analytical and economic sizing model based on the minimum levelized cost of energy, while Kamal [22] proposed a standalone rural microgrid model optimized using differential to reduce the overall cost of energy of the system.

However, there are other important aspects that should be considered in determining the optimal sizing of a microgrid. Liu *et al*. [11] considered the GHG emissions of diesel generators to formulate a multi-objective optimization problem for microgrid sizing. However, other components in the microgrid also contribute to GHG emissions throughout their lifecycle and should be considered. Boutros [23] proposed a modelling approach for the optimal sizing of an islanded microgrid that minimizes life-cycle carbon dioxide emissions as well as capital and operational expenses. Another study by Premadasa [24] proposed an optimization model for sizing and operating a hybrid energy system consisting of PV, wind energy, DG, and battery storage, aiming to minimize the total investment cost, operation and maintenance costs, and the system's carbon emissions. Another recent study by Zhu *et al*. [25] proposed a stochastic multi-objective sizing optimization model for microgrid planning with the aim to maximize the economic benefits and minimize carbon emissions. On the other hand, Mukhopadhyay and Das [26] considered line losses as one of the objective functions in grid-tied microgrid sizing. Based on these literatures, apart from cost, emissions and power losses are important aspects to be considered in determining the optimal sizing of a microgrid. For a standalone microgrid, power losses in power converters should be considered.

Based on the identified research gaps, this study proposes an Enhanced Rule-based EMS (ERB-EMS) for sizing a standalone microgrid consisting of PV, WT, DG, and battery storage. The ERB-EMS introduces the load shifting mechanism into RB-EMS. The proposed ERB-EMS is compared with RB-EMS approaches from other studies. A mathematical model based on LCOE, GHG emissions, and power losses of converters is proposed for microgrid sizing. The objective of microgrid sizing is to minimize all three objective functions. The Iterative-Pareto-Fuzzy (IPF) optimization method is employed to determine the optimum sizing of the microgrid.

The main contributions of this study are highlighted as follows:

- An ERB-EMS consisting of a day-ahead load shifting mechanism and RB-EMS is proposed in the study of microgrid sizing.
- A comparative analysis of the energy scheduling performance is conducted between the proposed ERB-EMS and the existing RB-EMSs (cycle charging and load following), highlighting the advantages of the ERB-EMS over the other two strategies.
- The sizing optimization results between different RB-EMS approaches (ERB-EMS, cycle charging, and load-following strategies) are studied.

## 2.0 MODELLING OF MICROGRID SYSTEM

When determining the optimum sizing of an isolated microgrid, selecting an appropriate EMS is crucial. The objective of microgrid sizing is to minimize the LCOE, GHG emissions, and internal power losses of microgrid components. Ouessant Island, a remote island in France that still relies on DG for power supply, is chosen as the study location. Figure 1 shows the proposed microgrid system. The system consists of PV, WT, battery storage, and a DG. The consumer load consists of two types: emergency load and responsive load. The emergency load must be met during each scheduling period, while the responsive load can be shifted to another period of time. A dump load is used to absorb excess power generation. An AC microgrid is considered in this study.

### 2.1 Diesel Generator

A DG is used as an alternative to the utility grid in some remote islands. The cost of fuel consumption by the DG at time $t$, $P_{DG,t}$ [27] is as follows:

$$DG_{Cost,t} = aP_{DG,t}^2 + bP_{DG,t} + c \quad (1)$$

where $a$, $b$, and $c$ are the DG cost coefficients, obtained from the DG fuel consumption curve. $P_{DG,t}$ represents the DG scheduled output power at time $t$.

### 2.2 PV Power

The power generation of the PV panels at time $t$, $P_{PV,t}$, depends on the hourly solar irradiance, $G_t$, and is calculated using (2):

$$P_{PV,t} = N_{PV} P_{STC} \left[ \frac{G_t}{G_{STC}} (1 - \gamma)(T_{c,t} - T_{STC}) \right] \quad (2)$$

Here, $G_{STC}$, $T_{STC}$, and $P_{STC}$ are the irradiance, temperature, and PV panel output power at standard test conditions, respectively. $\gamma$ is the temperature-dependent degradation coefficient and $N_{PV}$ denotes the number of PV panels.

### 2.3 WT Power

The power output of the WTs at time $t$, $P_{WT,t}$, is calculated based on the wind speed, $v_t$ and is shown in equation (3) [8]:

$$P_{WT,t} = N_{WT} \begin{cases} 0, & v_t < v_{ci} \\ P_{WT(rated)} \left( \frac{v_t - v_{ci}}{v_r - v_{ci}} \right)^3, & v_{ci} \le v_t < v_r \\ P_{WT(rated)}, & v_r \le v_t < v_{co} \\ 0, & v_t > v_{co} \end{cases} \quad (3)$$

where $v_{ci}$, $v_r$, and $v_{co}$ are the cut-in, rated, and cut-out wind speeds, respectively. $N_{WT}$ is the number of WTs and $P_{WT(rated)}$ is the rated power of the WTs.

### 2.4 Lithium-ion Battery

The charging and discharging rates of a battery affects its maximum charging and discharging power of the batteries ($P_{max(ch),t}$ and $P_{max(disch),t}$, respectively) [27] and are modeled as follows:

$$P_{max(ch),t} = I_{ch,t} N_{batt} E_{batt(rated)} \quad (4)$$

$$P_{max(disch),t} = I_{disch,t} N_{batt} E_{batt(rated)} \quad (5)$$

After a charging and discharging event, the energy state of battery changes, $E_{batt,t}$ is defined by (6).

$$E_{batt,t} = E_{batt,t-1} + \left( \eta_{ch,t} P_{batt(ch),t} - \frac{P_{batt(disch),t}}{\eta_{disch,t}} \right) \quad (6)$$

### 2.5 Enhanced Rule-based Energy Management System

This section discusses the operation of the proposed ERB-EMS, which consists of two steps. In the first step, a day-ahead load shifting mechanism is deployed to assess the feasibility of shifting load demand from peak hours to other hours. Then, in the second step, the RB-EMS is deployed for real-time energy scheduling.

One day prior to the actual energy distribution, the scheduling of responsive loads (RLs) shifting takes place. The mechanism determines the time, $t_s$, for shifting RLs based on forecasted PV, WT, and load demand data. The load shifting procedure is divided into Stage 1 and Stage 2, ensuring that the total RLs shifted within a day are fully recovered before the day ends.

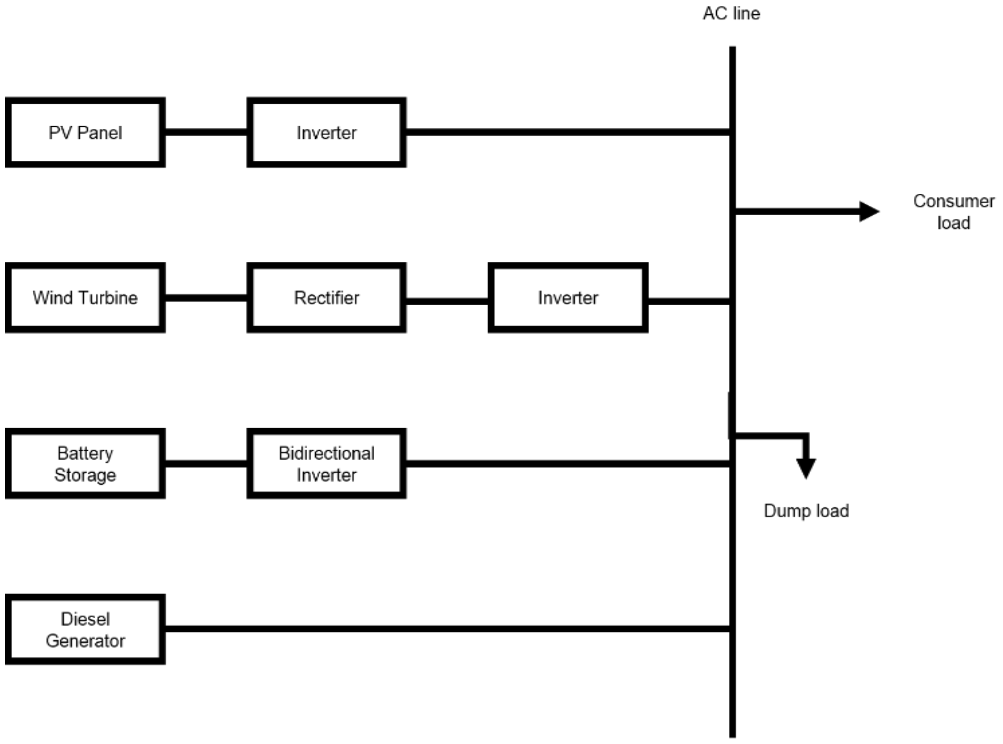


**Figure 1** Proposed microgrid configuration

In Stage 1, for each timestep, $t$, the system records the time, $t_R$, and the excess power generated, $P_R$, which can be utilized to recover any loads shifted during the scheduling period $T$, if the total power generated by the RESs, $P_{RES}$, during Stage 1 is greater than the total power demand, $P_{Demand}$. $P_R$ is constrained by the size of RL, $P_{R(max)}$. The accumulated extra power for the scheduling period T is then updated as $P_{R(total)}$.

Moving on to Stage 2, for each timestep, $t$, if the $P_{RES}$ is less than $P_{Demand}$, the system identifies the time when the RESs cannot fulfil the load demand and the amount of RLs to be shifted, $P_s$, based on the information collected from Stage 1. $P_s$ is subject to $P_{s(max)}$ and $P_{R(total)}$. $P_{s(max)}$ represents RLs' size. $P_{R(total)}$ is continually updated at each timestep to ensure all shifted power can be fully recovered by the end of the scheduling period. Figures 2 and 3 show the flowcharts of the proposed load-shifting mechanism for Stage 1 and Stage 2, respectively.

After DR program has been executed, the RB-EMS based on LF strategy will be implemented to perform energy scheduling based on the newly updated power demand. The proposed RB-EMS operates in two modes:

Mode I: When the generated power from RESs exceeds the power demand ($P_{extra} > 0$), the surplus power generated will be utilized to charge the battery, provided the battery power and capacity constraints are met. Otherwise, the excess power will be supplied to the dump load.

Mode 2: When the generated power from RESs is less than the power demand ($P_{extra} < 0$), the battery will be discharged to supply to the load, provided battery power and capacity constraints are satisfied. Otherwise, the DG will be activated if the constraints cannot be met.

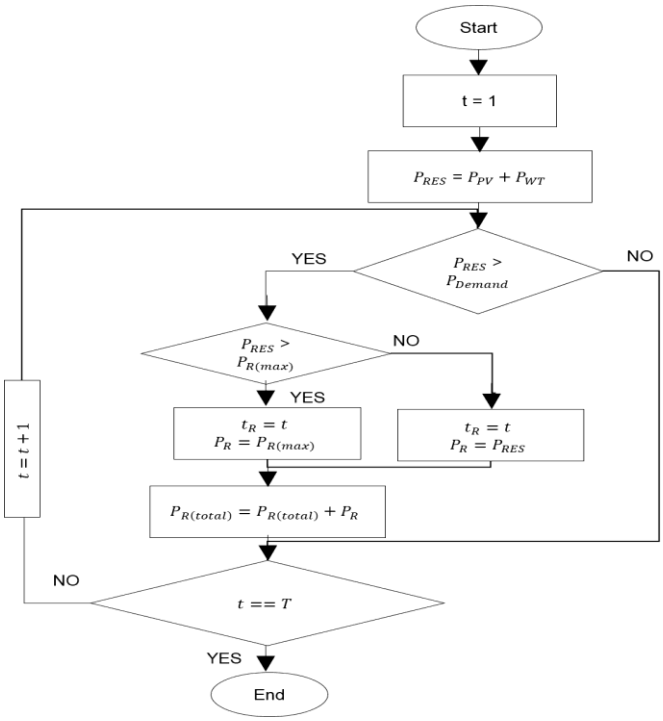


**Figure 2** Stage 1 of the proposed load shifting mechanism

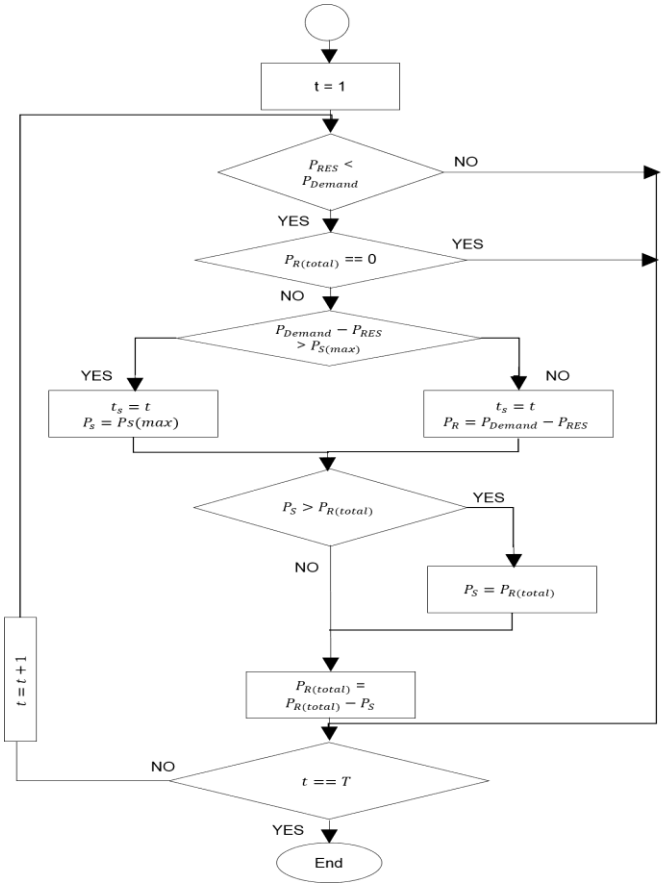


**Figure 3** Stage 2 of the proposed load shifting mechanism

## 2.6 Iterative-Pareto-Fuzzy Sizing Method

The IPF sizing method is used in this study to determine the size of the PV panels, WTs, and batteries that will give the minimum operating cost, penalty cost of GHG emissions, and annual internal energy losses. The PV–WT–battery size is first set to the minimum value. The size combination will then be used to run the EMS program, and all three costs will be calculated at the end of the program. The process is repeated by incrementally increasing the number of PV panels, WTs, and batteries. After the iteration process is completed, non-dominated solutions are obtained using Pareto analysis, and finally, the fuzzy satisfying method is applied to determine the best-compromised solution. Due to space constraint, the details on IPF method is explained in [14, 28]

## 2.7 Objective Function

This study aims to determine the optimum size of the PV–WT–battery combination that will minimize the LCOE, penalty cost of GHG emissions, and annual internal energy losses of power electronic converters (PECs) and batteries. The LCOE is the average cost per unit of energy generated, $F_{LCOE}$, and is calculated using (7):

$$F_{LCOE} = \frac{NPC}{\sum_{t=1}^{T} P_{demand,t}} \times CRF \tag{7}$$

Here, NPC and CRF represent the net present cost and capital recovery factor, respectively.

The penalty cost of GHG emissions includes the penalty costs due to $CO_2$-eq emissions of the DG, PV panels, WTs, and batteries. The total GHG emissions cost over the scheduling period $T$ calculated as:

$$F_{GHG} = \sum_{t=1}^{T} \begin{pmatrix} GHG_{PV,t} + GHG_{WT,t} + GHG_{DG,t} + \\ GHG_{Batt,t} \end{pmatrix} \tag{8}$$

The annual energy losses of PECs and batteries are considered as an objective function to be minimized and is given by:

$$F_{Loss} = \sum_{t=1}^{T} \begin{pmatrix} Loss_{PV-inv,t} + Loss_{WT-inv,t} + \\ Loss_{Batt-inv,t} + Loss_{roundtrip,t} \end{pmatrix} \tag{9}$$

where $Loss_{k,t}$ represents the power losses for component $k$ at time $t$.

## 3.0 RESULTS AND DISCUSSION

This section discusses the simulation results for the energy management strategy and sizing optimization. The simulation was conducted using MATLAB 2016 on a computer with the following specifications: Windows 8.1, 2.20 GHz 64-bit Intel Core i5-5200U processor.

The EMS is accessed over a one-year period. The load demand obtained is scaled according to the population density of the study area [29]. At the beginning of the first day, the battery capacity is assumed to be 0.90 of its rated capacity. The fixed DR incentive rate is set at 0.015 $/kWh. RLs is set at 20% of the load demand at each hour. The constant efficiency of the inverter is taken as 0.92, while the constant charging and discharging efficiency of battery is taken as 0.90.

Figure 4 shows the forecasted PV and WT generation for an ordinary day. Generally, PV power generation is available from $t$ = 10 to $t$ = 16, while the WT generation is rather unpredictable. The actual annual mean hourly PV generation is 0.899 kW, compared to the forecasted annual mean hourly PV generation of 0.994 kW. In contrast, the actual annual mean hourly WT generation is 6.23 kW, whereas the forecasted annual mean is 5.21 kW.

Figure 5 shows the forecasted and actual load demand data for an ordinary day [30, 31]. The actual mean hourly demand is 72.8 kW, while the forecasted mean hourly demand is 72.7 kW. Table 1 provides the technical data of the components used in this study. The power and energy rating shown in Table 1 represents the rating for a single unit of each component. A single PV unit has a rating of 5 kW, while a single WT unit has a power rating of 10 kW. As for the battery, a 24 kWh battery is used. DG is assumed to be installed before the study is conducted and it has a rating of 150 kW.

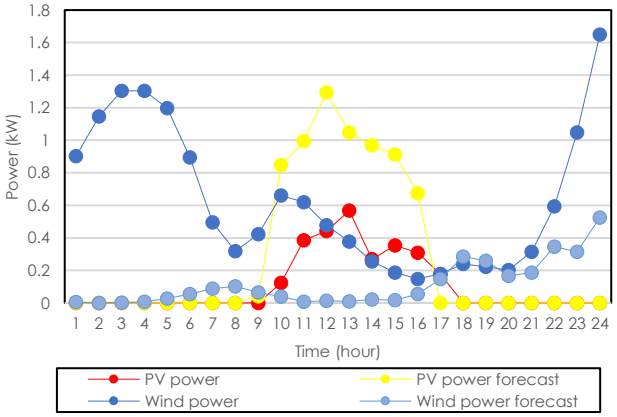


**Figure 4** Forecasted and actual power of a single PV and WT unit for an ordinary day

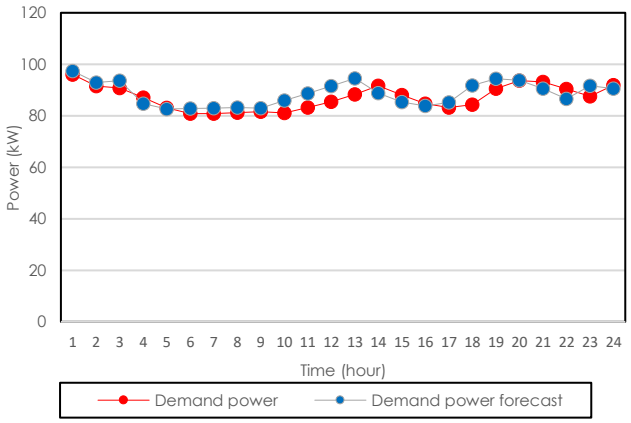


**Figure 5** Forecasted and actual power demand for an ordinary day

**Table 1** Technical data

| | |
|---|---|
| **Diesel Generator** | |
| *a, b, c* | −0.0007,0.667,0 |
| $Ci_{nv,DG}$ ($/kWh) | [32] |
| $C_{om,DG}$ ($/kWh/year) | 850 |
| $C_{rep,DG}$ ($/kWh) | 20 |
| Lifetime (year) | 800 |
| | 10 |
| $E_{GHG,DG}$ (kg CO2(equiv)/kWh) | 1.623 [33] |
| $P_{DG(min)}$, $P_{DG(max)}$ (kW) | 45, 150 |
| **Photovoltaic Panel** | |
| $P_{STC}$ (kW) | 5 |
| $C_{inv,PV}$ ($/kWh) | 1,350 [34] |
| $C_{om,PV}$ ($/kWh/year) | 17.8 [34] |
| $C_{rep,PV}$ ($/kWh) | 0 |
| Lifetime (year) | 20 |
| $E_{GHG,PV}$ (kg CO2(equiv)/kWh) | 0.05 [35] |
| γ (%/°C) | 0.005 |
| **Wind Turbine** | |
| $P_{WT(rated)}$ (kW) | 10 |
| $v_{ci}$, $v_{co}$, $v_r$ (m/s) | 2, 30, 9 |
| $C_{inv,WT}$ ($/kWh) | 1,515 [34] |
| $C_{om,WT}$ ($/kWh/year) | 50 [34] |
| $C_{rep,WT}$ ($/kWh) | 0 |
| Lifetime (year) | 20 |
| $E_{GHG,WT}$ (kg CO2(equiv)/kWh) | 0.007 |
| **Lithium-ion Battery** | |
| $E_{batt(rated)}$ (kWh) | 24 |
| $C_{inv,batt}$ ($/kWh) | 200 |
| $C_{om,batt}$ ($/kWh/year) | 6 |
| $C_{rep,batt}$ ($/kWh) | 180 |
| Lifetime (year) | 4 |
| $E_{GHG,Batt}$ (kg CO2(equiv)/kWh) | 0.7 [36] |

### 3.1 Operation of Microgrid Under Different RB-EMS Strategies

In this study, the operation of the microgrid with the implementation of ERB-EMS is analyzed and compared with two popular RB-EMS strategies in the existing literature, namely the CC and LF strategies. For

benchmarking purposes, the optimal size obtained when CC is implemented will be utilized to examine and compare the performance of microgrid operation under different RB-EMS strategies. The objective of sizing optimization is to minimize the LCOE, penalty cost of GHG emissions, and annual energy losses of PECs and batteries. The IPF method is employed to determine the optimal sizing. Table 2 presents the sizing optimization results when the CC method is implemented, with 22 PV units, 11 WT units and 5 battery units. Under the CC strategy, the LCOE obtained is 0.294 $/kWh, while the penalty cost of GHG emissions and annual energy losses are $4,586 and 84,332 kWh respectively. The annual operation shows that under this method, DG total output is 228,150 kWh while total energy supplied to the dump load is 280,418 kWh respectively. These values will be used to compare the performance of CC strategy with the other two strategies.

**Table 2** Sizing optimization results of microgrid when CC strategy is implemented

| Evaluation Metrics | Value |
|---|---|
| PV unit | 22 |
| WT unit | 11 |
| Battery unit | 5 |
| LCOE ($/kWh) | 0.294 |
| Penalty cost of GHG emissions ($) | 4,586.06 |
| Annual energy losses of PECs and batteries (kWh) | 84,332 |
| Dump energy (kWh) | 280,418 |
| DG contributions (kWh) | 228,150 |

The optimum sizes obtained are then used to evaluate the operation of the microgrid for CC, LF and ERB-EMS strategies. Figures 6, 7, and 8 depict the operation of the CC, LF, and ERB-EMS strategies, respectively, for an ordinary day (Day 100).

Based on Figure 6, when the CC method is applied, the batteries are prioritized for discharge when RES (PV and WT) generation is low (from $t$ = 6 to $t$ = 7, and from $t$ = 18 to $t$ = 19). From $t$ = 20 to $t$ = 24, when batteries are no longer able to discharge, the DG is turned on at rated power to cover the load demand. Excess power from the DG is then used to charge the battery or diverted to the dump load if batteries' storage is full.

In Figure 7, by using the LF strategies, from $t$ = 1 to $t$ = 8, the DG is operated at the minimum allowable power to cover the load deficit when RES generation is low and battery storage is unavailable. However, from $t$ = 21 to $t$ = 24, when the power deficit between the load demand and generation is too large, the DG generation is slightly increased above the minimum to just enough to cover the load demand. As a result of this operation, the total energy supplied by the diesel generator on this day is significantly reduced from 1200 kWh to 651.46 kWh. Additionally, the total energy supplied to the dump load has also dropped dramatically from 544.72 kWh to 78.20 kWh.

Figure 8 shows the proposed ERB-EMS shifts RLs when RES generation is low (from $t$ = 1 to $t$ = 9 and from $t$ = 17 to $t$ = 24) and recovers them when RES generation is abundant (from $t$ = 10 to $t$ = 16). This operation lowers the load demand during the period of low RES generation, allowing the DG remain running at minimum power throughout that period. Consequently, the DG generation for the day was further reduced to 540 kWh. Moreover, there is no power diverted to the dump load for that day, indicating that the power generation by microgrid components is fully utilized. This, in turn, explains the higher RES utilization of the system when ERB-EMS is applied. The comparison of annual performance for the LF and ERB-EMS strategies is shown in Table 3.

**Table 3** Annual performances of microgrid scheduling for LF and ERB-EMS strategies

| Evaluation metrics | LF | ERB-EMS |
|---|---|---|
| LCOE ($/kWh) | 0.213 | 0.199 |
| Penalty cost of GHG emissions ($) | 2,358 | 2,215 |
| Annual energy losses of PECs and batteries (kWh) | 69,940 | 72,716 |
| Dump energy (kWh) | 180,556 | 170,690 |
| DG contributions (kWh) | 120,902 | 106,373 |

Comparing Table 2 and Table 3, ERB-EMS provides the lowest LCOE (0.199$/kWh), penalty cost of GHG emissions ($2,215), and a significantly lower energy losses of PECs and batteries (72,716 kWh) compared to the CC strategy. Compared to the LF strategy, implementing ERB-EMS has successfully reduced the LCOE and penalty cost of GHG emissions by 6.57% and 6.06 %, respectively. The slightly higher annual energy losses of PECs and batteries result from the frequent charging and discharging of batteries, as ERB-EMS aims to minimize DG generation. Despite the 3.97% increase in annual energy losses, the percentage improvements in LCOE and GHG emissions are noteworthy trade-offs. The DR program in the ERB-EMS shifts RLs from periods of low RES generation to periods of high RES generation, allowing a larger amount of RES generation to be supplied to the load, and hence reducing DG power output to 106,373 kWh. Since the DG is the main contributor to cost and emissions, LCOE and GHG penalty cost are lowered when ERB-EMS is implemented.

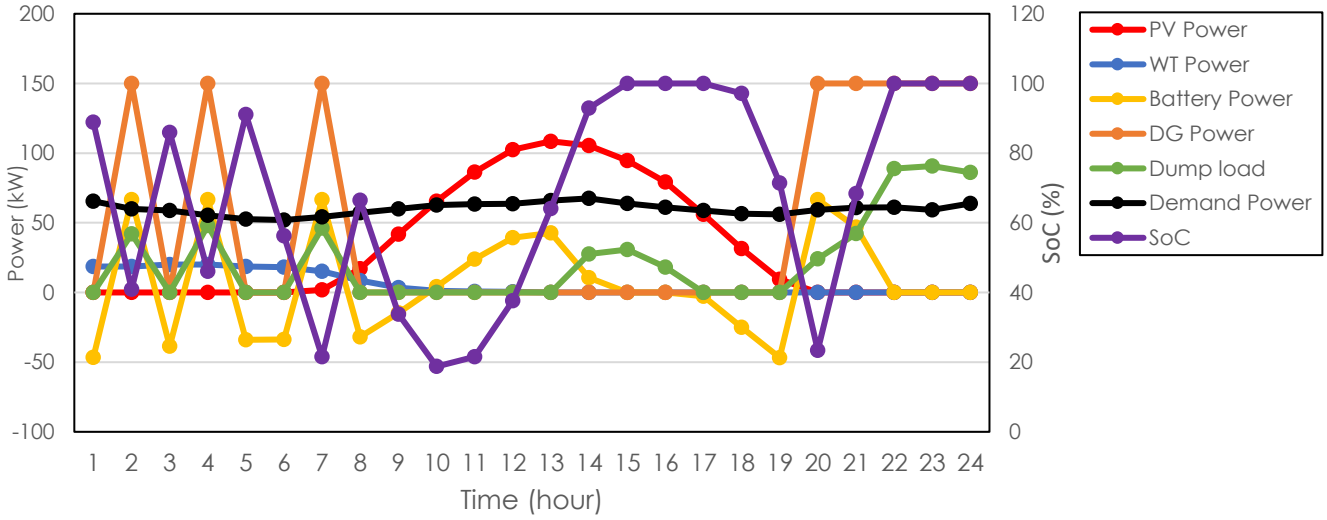


**Figure 6** Energy scheduling process when CC strategy is applied

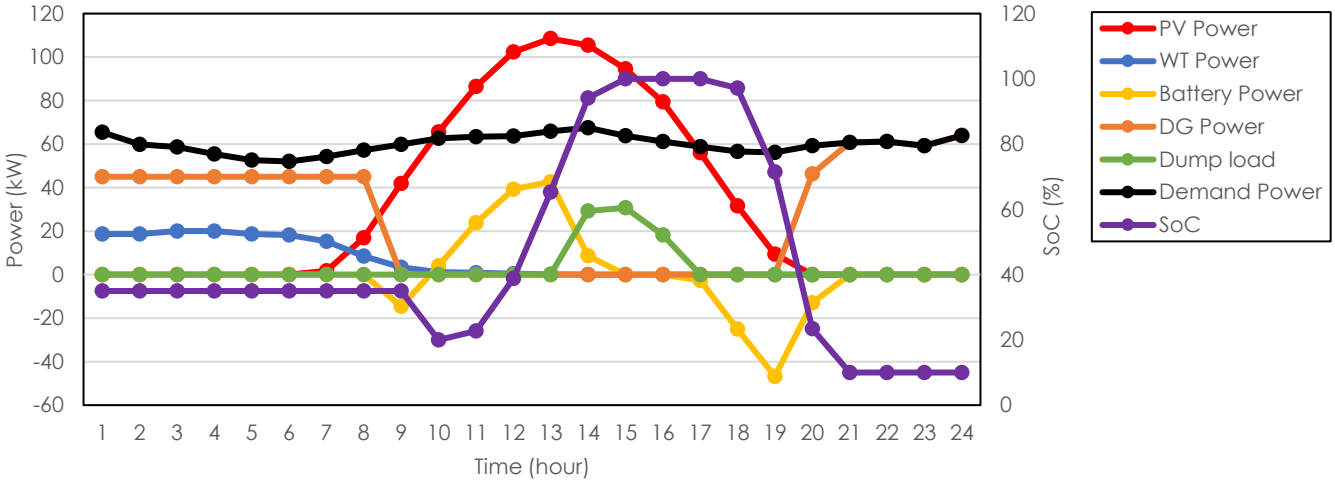


**Figure 7** Energy scheduling process when LF strategy is applied

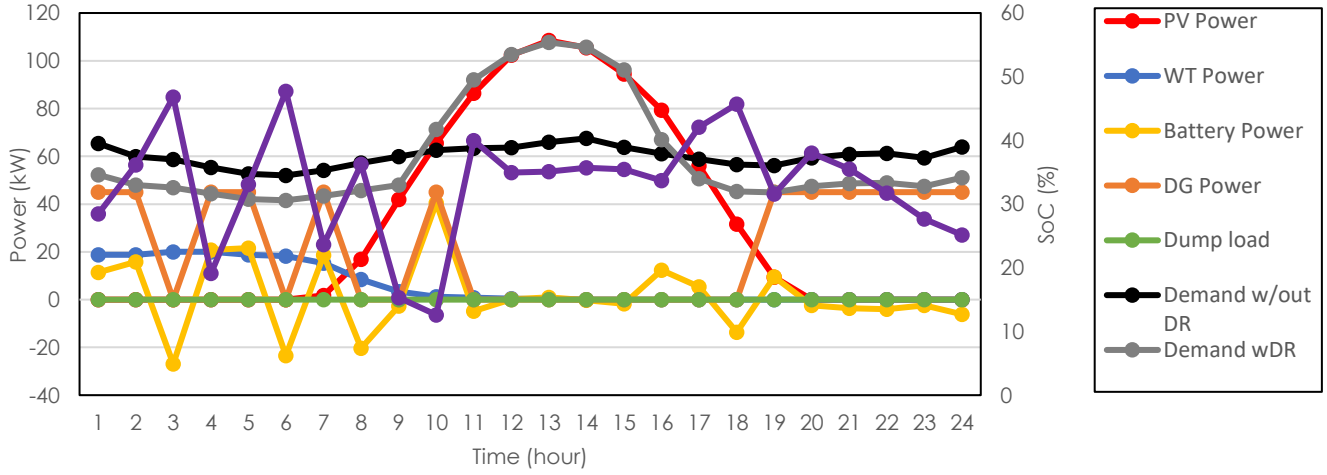


**Figure 8** Energy scheduling process when ERB-EMS is applied

### 3.2 Optimum Sizing of Microgrid Under Different RB-EMS Strategies

This section investigates the effect of RB-EMS on microgrid sizing. The optimum sizes for CC, LF, and ERB-EMS approaches are evaluated based on LCOE, penalty cost of GHG emissions, and annual energy losses. Table 2 in the previous subsection presented the optimum size when the CC strategy is applied, while Table 4 in this subsection presents the optimum sizes for the LF and ERB-EMS strategies.

**Table 4** Comparison between sizes and objective functions obtained for different RB-EMSs

| RB-EMS | Optimum Sizes | | | Objective Functions | | |
|---|---|---|---|---|---|---|
| | PV | WT | Battery | LCOE ($/kWh) | Penalty cost of GHG emissions ($) | Annual energy losses (kWh) |
| LF | 22 | 11 | 3 | 0.216 | 2,365 | 67,106 |
| ERB-EMS | 24 | 11 | 2 | 0.205 | 2,220 | 69,537 |

Comparing Table 2 and Table 4, since ERB-EMS operates by shifting excess RES generation, the optimum PV size obtained is slightly higher to further reduce the DG power output and increase PV power utilization. Despite this, the calculated LCOE is the lowest at $0.205, compared to $0.294 for the CC strategy and $0.216 for the LF strategy. As a results, the GHG emissions is also the lowest, with the penalty cost of $ 2,220, when ERB-EMS is applied. However, a larger PV size results in a greater amount of power conversion, leading to higher energy losses by 3.50%.

## 4.0 CONCLUSION

In conclusion, this paper introduces an ERB-EMS for optimizing the sizing of a standalone microgrid. To assess its effectiveness, the proposed strategy was benchmarked against other RB-EMS approaches, using sizing results and objective function values as metrics.

The scheduling performance based on the optimal sizes obtained from the CC strategy demonstrates that the proposed ERB-EMS achieves the lowest DG contributions and dump energy compared to the CC and LF strategies. The decrease in DG power output by 53.7% compared to the CC strategy and 12.0% compared to the LF strategy indicates that ERB-EMS successfully minimizes DG dependency, thereby increasing RES utilization.

A comparison of the optimum sizing obtained by CC, LF, and ERB-EMS strategies shows that, despite a slightly larger optimal size, ERB-EMS yields the lowest LCOE and GHG penalty cost at $0.205/kWh and $2,220, respectively. The larger PV size further reduces DG power dependency.

One of the major limitations of this work is that the proposed load shifting mechanism must be evaluated one day ahead before the real time energy scheduling. Therefore, in the future, a real time load shifting mechanism will be proposed to enhance the system's suitability for practical application.

## Acknowledgement

This work is funded by the Ministry of Higher Education under Fundamental Research Grant Scheme (FRGS/1/2021/TK0/UTM/02/20).

## Conflicts of Interest

The author(s) declare(s) that there is no conflict of interest regarding the publication of this paper.

## References

[1] United Nation Environment Programme. 2022. (UNEP). Facts about the Climate Emergency. https://www.unep.org/explore-topics/climate-action/facts-about-climate-emergency (accessed Nov. 13, 2022).

[2] Raya-Armenta, J. M., Bazmohammadi, N., Avina-Cervantes, J. G., Sáez, D., Vasquez, J. C., and Guerrero, J. M. 2021. Energy Management System Optimization in Islanded Microgrids: An Overview and Future Trends. *Renewable and Sustainable Energy Reviews.* 149.

[3] Lara, J. D., Olivares, D. E., and Canizares, C. A. 2019. Robust Energy Management of Isolated Microgrids. *IEEE Systems Journal.* 13(1): 680–691.

[4] Shi, Z., Liang, H., Huang, S., and Dinavahi, V. 2019. Distributionally Robust Chance-constrained Energy Management for Islanded Microgrids. *IEEE Transactions on Smart Grid.* 10(2): 2234–2244.

[5] Salazar, A., Berzoy, A., Song, W., and Velni, J. M. 2020. Energy Management of Islanded Nanogrids through Nonlinear Optimization Using Stochastic Dynamic Programming. *IEEE Transactions on Industry Applications.* 56(3): 2129–2137.

[6] Javidsharifi, M., Niknam, T., Aghaei, J., Shafie-khah, M., and Catalao, J. P. S. 2020. Probabilistic Model for Microgrids Optimal Energy Management Considering AC Network Constraints. *IEEE Systems Journal.* 14(2): 2703–2712.

[7] Arkhangelski, J., Abdou-Tankari, M., and Lefebvre, G. 2021. Day-Ahead Optimal Power Flow for Efficient Energy Management of Urban Microgrid. *IEEE Transactions on Industry Applications.* 57(2): 1285–1293.

[8] Bukar, A. L., Tan, C. W., Yiew, L. K., Ayop, R., and Tan, W. S. 2020. A Rule-based Energy Management Scheme for Long-term Optimal Capacity Planning of Grid-independent Microgrid Optimized by Multi-objective Grasshopper Optimization Algorithm. *Energy Conversion and Management.* 221: 113161.

[9] Fathy, A., Kaaniche, K., and Alanazi, T. M. 2020. Recent Approach based Social Spider Optimizer for Optimal Sizing of Hybrid PV/Wind/Battery/Diesel Integrated Microgrid in Aljouf Region. IEEE Access. 8: 57630–57645.

[10] Shezan, S. A. 2020. Design and Demonstration of an Islanded Hybrid Microgrid for an Enormous Motel with the Appropriate Solicitation of Superfluous Energy by Using iHOGA and MATLAB. *International Journal of Energy Research.* 45(4): 5567–5585.

[11] Liu, H., Wang, S., Liu, G., Zhang, J., and Wen, S. 2020. SARAP Algorithm of Multi-objective Optimal Capacity

Configuration for WT-PV-DE-BES Stand-Alone Microgrid. *IEEE Access*. 8: 126825–126838.
[12] Zhou, Z., and L. Ge. 2019. Operation of Stand-Alone Microgrids Considering the Load Following of Biomass Power Plants and the Power Curtailment Control Optimization of Wind Turbines. *IEEE Access*. 7: 186115–186125.
[13] Abdelsattar, M., Mesalam, A., Diab, A.A.Z., Fawzi, A., and Hamdan, I. 2024. Optimal Sizing of a Proposed Stand-alone Hybrid Energy System in a Remote Region of Southwest Egypt Applying Different Meta-heuristic Algorithms. *Neural Computing and Applications*. 36(26): 16251–16269.
[14] Mukhtaruddin, R. N. S. R., Rahman, S. A., Hassan, M. Y., and Jamian J. J. 2015. Optimal Hybrid Renewable Energy Design in Autonomous System using Iterative-Pareto-Fuzzy technique. *International Journal of Electrical Power & Energy Systems*. 64: 242–249.
[15] Alsharif, A., Tan, C. W., Ayop, R., Lau, K. Y., and Dobi, A. M. 2021. A Rule-based Power Management Strategy for Vehicle-to-Grid System using Antlion Sizing Optimization. *Journal of Energy Storage*. 41: 102913.
[16] Hakimi, S. M., Hasankhani, A., Shafie-khah, M., Lotfi, M., and Catalão, J. P. S. 2022. Optimal Sizing of Renewable Energy Systems in a Microgrid Considering Electricity Market Interaction and Reliability Analysis. *Electric Power Systems Research*. 203: 107678.
[17] Mohandes, B., Acharya, S., Moursi, M. S. E., Al-Sumaiti, A. S., Doukas, H., and Sgouridis, S. 2020. Optimal Design of an Islanded Microgrid with Load Shifting Mechanism Between Electrical and Thermal Energy Storage Systems. *IEEE Transactions on Power Systems*. 35(4): 2642–2657.
[18] Mukhopadhyay, B., and Das, D. 2021. Optimal Multi-Objective Expansion Planning of a Droop-regulated Islanded Microgrid. *Energy*. 218.
[19] Candra, O, Ahmed, O. A., Alzubaidi, L. H., Sharma, M. K., Rodriguez-Benites, C., and Mude, I. S. 2024. Optimal Planning of the Microgrid Considering Optimal Sizing of the Energy Resources. *International Journal of Applied and Computational Mathematics*. 10(3): 115.
[20] Zhu, W., Guo, J., Zhao, G., and Zeng, B. 2020. Optimal Sizing of an Island Hybrid Microgrid Based on Improved Multi-Objective Grey Wolf Optimizer. *Processes*. 8(12).
[21] Khawaja, Y., Qiqieh, I., Alzubi, J., Alzubi, O., Allahham, A., and Giaouris, D. 2023. Design of Cost-based Sizing and Energy Management Framework for Standalone Microgrid using Reinforcement Learning. *Solar Energy*. 251: 249–260.
[22] Kamal, M. M., Ashraf, I., and Fernandez, E. 2023. Optimal Sizing of Standalone Rural Microgrid for Sustainable Electrification with Renewable Energy Resources. *Sustainable Cities and Society*. 88: 104298.
[23] Boutros, F., Doumiati, M., Olivier, J. C., Mougharbel, I., and Kanaan, H. 2023. New Modelling Approach for the Optimal Sizing of an Islanded Microgrid Considering Economic and Environmental Challenges. *Energy Conversion and Management*. 277: 116636.
[24] Premadasa, P. N. D., Silva, C. M. M. R. S., Chandima, D. P., and Karunadasa, J. P. 2023. A Multi-objective Optimization Model for Sizing an Off-grid Hybrid Energy Microgrid with Optimal Dispatching of a Diesel Generator. *Journal of Energy Storage*. 68: 107621.
[25] Zhu, X., Ruan, G., Geng, H., Liu, H., Bai, M., and Peng, C. 2024. Multi-Objective Sizing Optimization Method of Microgrid Considering Cost and Carbon Emissions. *IEEE Transactions on Industry Applications*. 60(4): 5565–5576.
[26] Mukhopadhyay, B., and Das, D. 2022. Optimal Multi-Objective Long-term Sizing of Distributed Energy Resources and Hourly Power Scheduling in a Grid-tied Microgrid. *Sustainable Energy, Grids and Networks*. 30: 100632.
[27] Zia, M. F., Elbouchikhi, E., Benbouzid, M., and Guerrero, J. M. 2019. Energy Management System for an Islanded Microgrid with Convex Relaxation. *IEEE Transactions on Industry Applications*. 55(6): 7175–7185.
[28] Ibrahim, N. N., Jamian, J. J., and Rasid, M. M. 2024. Optimal Multi-objective Sizing of Renewable Energy Sources and Battery Energy Storage Systems for Formation of a Multi-microgrid System Considering Diverse Load Patterns. *Energy*. 304: 131921.
[29] Insee. 2022. Legal populations 2019 - Municipality of Ouessant (29155). Available: https://www.insee.fr/fr/statistiques/6005800?geo=COM-29155.
[30] Nasa Power. 2020. Data Access Viewer. Available: https://power.larc.nasa.gov/data-access-viewer/.
[31] RTE. 2020. eCO2mix - Electricity consumption in France. Available: https://www.rte-france.com/en/eco2mix/electricity-consumption-france#.
[32] General Power. 150KW Cummins Generator. Available: https://www.genpowerusa.com/diesel-generators/150-kw-cummins-generator-188-kva-three-phase-genpowerusa-gp-c150-60t3/.
[33] Somorin, T. O., Di Lorenzo, G., and Kolios, A. J. 2017. Lifecycle Assessment of Self-generated Electricity in Nigeria and Jatropha Biodiesel as an Alternative Power Fuel. *Renewable Energy*. 113: 966–979.
[34] IRENA. 2021. Renewable Power Generation Costs in 2020.
[35] Milousi, M., Souliotis, M., Arampatzis, G., and Papaefthimiou, S. 2019. Evaluating the Environmental Performance of Solar Energy Systems through a Combined Life Cycle Assessment and Cost Analysis. *Sustainability*. 11(9).
[36] Liang, Y. 2017. Life Cycle Assessment of Lithium-ion Batteries for Greenhouse Gas Emissions. *Resources, Conservation and Recycling*. 117: 285–293.